

# Preparation and In Vitro Evaluation of Imiquimod Loaded Polylactide-based Micelles as Potential Vaccine Adjuvants

Gloria Jiménez-Sánchez · Vincent Pavot · Christelle Chane-Haong · Nadège Handké · Céline Terrat · Didier Gigmes · Thomas Trimaille · Bernard Verrier

Received: 20 May 2014 / Accepted: 24 July 2014  
© Springer Science+Business Media New York 2014

## ABSTRACT

**Purpose** Activation of immune cells through pattern recognition receptors (PRRs), such as Toll-like receptors (TLRs) or NOD-like receptors (NLRs), has been identified as a key issue in the development of new efficient vaccine adjuvants. We report here on the elaboration and immunostimulatory potential of polylactide (PLA)-based micelles core-loaded with imiquimod TLR7 ligand and able to be further surface-functionalized with antigenic protein (HIV-1 Gag p24) for antigen delivery purpose.

**Methods** Micelles prepared from poly(D,L-lactide)-b-poly(N-acryloxysuccinimide-co-N-vinylpyrrolidone) amphiphilic copolymer were incubated in the presence of imiquimod, leading to 1.2 wt% loading, and further conjugated to p24 antigen through reaction of p24 lysines and N-terminal amine with the N-succinimidyl pendant groups of the micelle corona. The impact of imiquimod encapsulation in the micelles on its immunostimulatory properties was investigated *in vitro*, by monitoring: (i) the NF- $\kappa$ B and mitogen-activated protein kinases (MAPK) pathways through experiments with RAW-Blue™ cells, a mouse macrophage cell line encoding an NF- $\kappa$ B/AP-1 inducible reporter construct; (ii) human dendritic cells (DCs) maturation markers by flow cytometry.

**Electronic supplementary material** The online version of this article (doi:10.1007/s11095-014-1465-5) contains supplementary material, which is available to authorized users.

G. Jiménez-Sánchez · V. Pavot (✉) · C. Chane-Haong · C. Terrat · B. Verrier  
Université Lyon 1, CNRS, UMR 5305, Biologie Tissulaire et Ingénierie Thérapeutique, IBCP  
7 Passage du Vercors, 69367 Lyon Cedex 07, France  
e-mail: vincent.pavot@gmail.com

N. Handké · D. Gigmes · T. Trimaille (✉)  
Aix-Marseille Université, CNRS, UMR 7273, Institut de Chimie Radicalaire, Avenue Escadrille Normandie-Niemen,  
13397 Marseille Cedex 20, France  
e-mail: thomas.trimaille@univ-amu.fr

**Results** RAW-Blue™ cells based experiments showed that imiquimod encapsulated in the micelles was much more efficient to activate the NF- $\kappa$ B and MAPK pathways than free imiquimod. Furthermore, encapsulated imiquimod was found to induce much higher maturation of DCs than the free analog. Finally, these immunostimulatory properties of the loaded imiquimod were shown to be conserved when the p24 antigen was coupled at the micelle surface.

**Conclusions** Taken together, these data regarding improved immunostimulatory efficiency suggest the strong potential of our micelle-based nano-system for vaccine delivery.

**KEY WORDS** dendritic cell maturation · imiquimod · immunostimulation · polylactide-based micelles · vaccine

## INTRODUCTION

With the recent advances in genomics and proteomics, a wide variety of potential target antigens (recombinant proteins, synthetic peptides or DNA) are now available for the development of subunit vaccines, which are a promising alternative to traditional vaccines obtained from attenuated or inactivated pathogens regarding safety concerns. However, antigens are often poorly immunogenic when administered alone without adjuvants. Until recently, hydroxide and phosphate salts of aluminium and calcium, and among them alum, were the only adjuvants licensed for human use (1). Whereas aluminium compounds have been used with a large number of antigens, these adjuvants are not suitable for all antigens and are insufficient in many respects, including variable or poor adsorption of some antigens, the difficulty to lyophilize, the general requirement for booster doses, the rare occurrence of hypersensitivity reactions in some subjects and the inability to elicit cytotoxic T-cell (CTL) responses and to elicit mucosal IgA antibody responses (2).

Consequently, over the last decade, significant research efforts have been devoted to the development of new, improved vaccine delivery systems, such as liposomes (3), emulsions (MF59, AS02) (4) or solid polymer nanoparticles (5). Among the latter biodegradable polylactide/poly(lactide-co-glycolide) (PLA/PLGA) based nanoparticles (NPs) represent safe systems and have been extensively described for delivery of encapsulated (6) or surface-adsorbed antigens (7), and can provide systemic antibody titers comparable to those of aluminium salts (8,9).

It has been now well-established that activation of immune cells through pattern recognition receptors (PRRs), such as Toll-like receptors (TLRs), NOD-like receptors (NLRs) or C-type lectins (CLRs), play a key role in the development of potent and oriented immune responses (10,11). Targeting PRRs with adjuvants bearing appropriate ligands appears thus a valuable approach (12), and several works focused on the incorporation of these “danger signal” molecules to PLGA/PLA based NPs, either by encapsulation (monophosphoryl lipid A (MPL) (6), chemical mimetic RC529 (13), poly(I:C) (14), CpG (15), NOD1 and/or NOD2 ligands (7)) or by surface coupling (typically mannose (16)). Among PRRs ligands, imiquimod is a molecule of the imidazoquinoline family, acting as a ligand of the intracellular endosomal TLR7, which is already approved as a 5% cream (Aldara, 3M Pharmaceuticals) for the treatment of genital warts (17,18). The mechanism of action of imiquimod proceeds, at least in part, through activation of the NF- $\kappa$ B pathway, leading to further dendritic cell (DC) maturation and production of pro-inflammatory cytokines (19), a fundamental step towards effective immune response. As the molecule is hydrophobic and its receptor is intracellular, there is interest for its encapsulation in polymeric NPs, which could avoid premature degradation and favor delivery into the cytoplasm, as recently reported for PLGA NPs (6) and pH-sensitive dextran based NPs (20). In previous works, we have designed a versatile PLA-based micelle platform which allows core/corona functionalization with hydrophobic/hydrophilic molecules, through the hydrophobic PLA core and the presence of *N*-succinimidyl ester reactive groups in the poly(*N*-vinylpyrrolidone) (PNVP)-based corona, and showed their potential interest for drug/vaccine delivery (21). Moreover, this copolymer, when used as a surfactant at the surface of PLA NPs, was previously shown in our group to be non-cytotoxic (DC cells) (22), supporting earlier studies on PLA-*b*-PNVP based copolymers regarding biocompatibility (23,24).

Small NPs such as micelles (~100 nm or less) have been very little explored for vaccine purpose but emerging works tend to prove the relevancy of such nano-carriers for antigen delivery (25–27). One of the explanations is that so small particles do not limit to association with DCs from the injection site, but are more readily to drain to the lymph nodes, where DCs are present in larger amounts. We show in this

study that micelles loaded with imiquimod significantly potentialize the immuno-modulatory properties of this molecule, while presenting at their surface the antigen to deliver.

## MATERIALS AND METHODS

### Materials

The poly(D,L-lactide)-*b*-poly(*N*-acryloxysuccinimide-co-*N*-vinylpyrrolidone) (PLA-*b*-P(NAS-co-NVP)) block copolymer (19,000 and 22,000 g.mol<sup>-1</sup> for PLA and P(NAS-co-NVP), respectively; NAS/NVP molar ratio: 53/47, PDI=1,6) was synthesized as previously described (21). Imiquimod (>98%) was from TCI America. p24 protein was purchased from PX Therapeutics (France, 2.4 mg.mL<sup>-1</sup> in PBS, pH 7.4, Mw=24 kDa).

### Micelle Preparation

Five milliliters of a copolymer solution in acetonitrile (10 mg.mL<sup>-1</sup>) were added to 10 mL of milli-Q water, under agitation (200 rpm), allowing the formation of micelles. Acetonitrile was removed by evaporation under reduced pressure. The micelle concentration was determined by measuring the solid content, after heating the micellar solution to constant weight in an oven at 70°C for 24 h. Final micelle concentration was typically 5.2 mg.mL<sup>-1</sup>.

### Micelle Size and Zeta Potential

The hydrodynamic diameter of the micelles, diluted 1/100 in a 1 mM solution of NaCl, was measured by dynamic light scattering at 25°C using a Zetasizer Nano ZS90 apparatus (Malvern, UK). The diameters were the result of the average of three measurements. Electrophoretic mobilities were measured on the same diluted samples at 25°C and were converted to zeta potential according to the Smoluchowski's equation. The values were the mean of four measurements.

### Imiquimod Loading

Two milliliters of micelle solution (5.2 mg.mL<sup>-1</sup> in water) were incubated at 20°C with 1 mg of imiquimod. A control with water (instead of the micelle solution) and the same mass of imiquimod was also incubated. Both suspensions were under agitation, and a centrifugation was performed (Eppendorf centrifuge model 5418, 5 min at 1,380×*g*) at different times (1 h, 2 h, 27 h, 70 h) to remove the imiquimod powder non solubilized in the micelles. The solution was analyzed by UV spectroscopy (Infinite M1000, Tecan, UV transparent 96-well microplates star Greiner) after dilution by a factor of 10 in water.

To quantify the encapsulated imiquimod, the micelle solution was 10-fold diluted in DMSO to destroy the micelles by solubilization of the copolymer. The absorbance of imiquimod ( $\lambda_{\text{max}} = 318 \text{ nm}$ ) was measured and related to the imiquimod concentration using a calibration curve of absorbance *versus* the concentration of imiquimod, previously evaluated under the same conditions (DMSO/water: 9/1 v/v).

### HIV-1 p24 Micelle Functionalization

The coupling of p24 protein at the micellar surface was performed by adding a volume (typically 300  $\mu\text{L}$ ) of micelle suspension ( $5.2 \text{ mg.mL}^{-1}$ ), with or without encapsulated imiquimod, to the same volume of p24 in PBS (pH 7.4) at concentrations of  $0.6 \text{ mg.mL}^{-1}$  (concentrations in the coupling medium:  $2.6 \text{ mg.mL}^{-1}$  for the micelles and  $0.3 \text{ mg.mL}^{-1}$  for the protein p24). The samples were allowed to stir at room temperature for 20 h.

### p24 Coupling Characterization

SDS-PAGE (sodium dodecyl sulfate polyacrylamide gel electrophoresis) was used to discriminate the p24 coupled to micelles from the free p24 using an electrophoresis equipment Bio-Rad. The concentration gel was 4% and the separation gel 15% final enacryl/bisacrylamide. The micelle aqueous solutions (with or without encapsulated imiquimod and with the p24 coupled at the surface) were mixed with the carrier buffer (Laemmli Sample 5 $\times$  Buffer: 300 mM Tris-Cl pH 6.8, 10% SDS, 40% glycerol, 10 mM dithiothreitol, 0.05% bromophenol-blue) (micelle/carrier buffer: 4/1 v/v). The migration was carried out at 100 V for 10 min and at 200 V for 40 min. Both gels (separation and concentration) were used for revelation. The gels were further stained with Coomassie blue. The free p24 (at the same concentration as in the micelle solution) and the micelles without p24 were used as a control. The amino group analysis was determined by the 2,4,6-trinitrobenzenesulfonic acid (TNBS) method, as previously described (28). Briefly, 10  $\mu\text{L}$  of p24-micelle or p24 solutions were mixed with 10  $\mu\text{L}$  of TNBS solution (1.7 mM in water) in 80  $\mu\text{L}$  of sodium borate buffer (0.1 M, pH 9.5) and incubated at 37°C for 1 h. The absorbance was measured at 344 nm using the Infinite M1000 Tecan spectrometer. p24 solutions of known concentrations in the coupling conditions (PBS) but without micelles were used as reference.

### Imiquimod Release from Micelles

1.9 mL of imiquimod loaded micelles (surface-functionalized or not with p24) were placed in a dialysis bag (cut-off 3500) and dialyzed against 19 mL PBS (pH 7.4) or sodium acetate buffer 0.3 M (pH 5) at 37°C. The latter concentration was chosen to ensure a ionic strength value similar to that of PBS.

At predetermined times, the buffer media were renewed (19 mL each time). Quantification of imiquimod in buffer media was performed by reverse phase HPLC (Agilent 1100) using a Merck column (LiChroCART, C18, 5  $\mu\text{m}$ , 125 $\times$ 4 mm), with eluent composed of water/acetonitrile 70/30 (v/v) with 0.1% TFA at a flow rate of  $0.8 \text{ mL.min}^{-1}$ . Imiquimod was detected at 244 nm.

### *In Vitro* Evaluation of the TLR7 Pathway Activation in the RAW-Blue Cell Line

RAW-Blue<sup>TM</sup> cells (InvivoGen) are derived from RAW 264.7 macrophages. They stably express a secreted embryonic alkaline phosphatase (SEAP) gene inducible by NF- $\kappa$ B and AP-1 transcription factors. RAW-Blue<sup>TM</sup> cells express all TLRs (with the exception of TLR5) as well as RIG-I, MDA-5, NOD1 and NOD2. The presence of specific agonists of these receptors induces signalling pathways leading to the activation of NF- $\kappa$ B and AP-1. Upon TLR stimulation, RAW-Blue<sup>TM</sup> cells activate NF- $\kappa$ B and/or AP-1 leading to the secretion of SEAP which is easily detectable and measurable when using QUANTI-Blue<sup>TM</sup> (InvivoGen), SEAP detection medium. Antibiotic pressure with Zeocin<sup>TM</sup> is required to maintain the plasmid coding for SEAP.

Free or encapsulated imiquimod was cultured with RAW-Blue<sup>TM</sup> Cells at final concentrations ranging from 0 to  $1 \mu\text{g.mL}^{-1}$  in 96-microwell plates (100,000 cells/well in duplicate) for 21 h at 37°C in a 5% CO<sub>2</sub> incubator. For this purpose, 20  $\mu\text{L}$  of free or micelle encapsulated imiquimod solution (at concentrations from 0 to  $10 \mu\text{g.mL}^{-1}$  in PBS pH 7.4) were added to 180  $\mu\text{L}$  of cells. Free imiquimod solutions prepared by successive PBS dilutions of an imiquimod stock solution in sodium acetate pH 5 ( $90 \mu\text{g.mL}^{-1}$ ) due to poor solubility of imiquimod at pH 7.4. Then 50  $\mu\text{L}$  of induced RAW-Blue<sup>TM</sup> cells supernatant were added to 150  $\mu\text{L}$  of resuspended QUANTI-Blue<sup>TM</sup> in a flat-bottom 96-well plate and incubate at 37°C for 90 min. The absorbance of the samples was then measured at 620 nm using a microplate reader (Bio-Rad) to determine the SEAP levels.

### *In Vitro* Maturation of Human Monocyte Derived DCs (MoDCs)

Monocytes were purified from peripheral human blood, obtained from EFS (Etablissement Français du Sang) by density gradient centrifugations using Ficoll-Paque<sup>TM</sup> plus and Percoll (GE Healthcare). Remaining erythrocytes, NK, B- and T-cells were then depleted by anti-glycophorin A, anti-CD56, anti-CD19 and anti-CD3 antibodies (Beckman Coulter) respectively, using Dynabeads<sup>®</sup> Pan Goat antimouse IgG (Invitrogen). Purified monocytes ( $0.5 \times 10^6 \text{ cell.mL}^{-1}$ ) were then cultured in RPMI medium supplemented with 10% heat-inactivated fetal calf serum (FCS), gentamycin

(50 U.mL<sup>-1</sup>), 100 U.mL<sup>-1</sup> penicillin and 100 µg.mL<sup>-1</sup> streptomycin in the presence of 62.5 ng.mL<sup>-1</sup> of human interleukin-4 (IL-4) (R&D systems) and 75 ng.mL<sup>-1</sup> of human granulocyte macrophage colony stimulating factor (GM-CSF) (Collaborative Biomedical Product-Bioscience) to differentiate into MoDCs. After 6 days, empty micelles, free or encapsulated imiquimod (diluted in the cell culture medium at 5 µg.mL<sup>-1</sup>), were added to 1 million of differentiated MoDCs for 48 h and incubated at 37°C, 5% CO<sub>2</sub>. DCs only cultured in complete RPMI medium were used as a negative control of stimulation, and those cultured in presence of 2.5 µg.mL<sup>-1</sup> of LPS were used as a positive control. DCs maturation was assessed by cell surface immunostaining using monoclonal antibodies against lineage markers and co-stimulatory molecules. Cells were stained with APC-labeled anti-CD1a (dendritic cells marker), and PE-labeled anti-CD80, -CD83 or -CD86. The isotype controls were IgG1 and IgG2a (BD Pharmingen™). Ten thousand events were acquired by Fluorescence Activated Cell Sorting (FACS) with a FACS Canto I (Tour Inserm CERVI, Lyon), and the data were analyzed using the FlowJo software.

### Statistical Data Analyses

Analyses were performed using SigmaPot™ software, version 11.0. Statistical data analyses were performed using analysis of variance ANOVA with Bonferroni's post test for comparison of pairs. Statistical significances were indicated on the figures. \*\*\**P*<0.001, \*\**P*<0.01, \**P*<0.05.

## RESULTS AND DISCUSSION

### Micelle Formation and Imiquimod Loading

Our approach to prepare the imiquimod/p24 decorated micelles relied on post-encapsulation (imiquimod) and post-conjugation (p24 protein) on the prepared PLA-b-P(NAS-co-NVP) block copolymer micelles (Fig. 1). The copolymer micelles were prepared by the common solvent (or nanoprecipitation) method, by dissolving the copolymer in acetonitrile, following by addition in water. The micelle mean size determined from dynamic light scattering (DLS) was 56.5 ± 2.0 nm (polydispersity index (PI) of 0.05), and critical micellar concentration, determined by the Nile Red probe method (as previously described (21)) was 20 mg.L<sup>-1</sup>. The micelle solution was incubated under stirring with the imiquimod powder. The micelle solution was then simply washed from the non soluble imiquimod powder by centrifugation. As a control, pure water solution was also incubated with imiquimod following the same process, to evaluate the fraction of the product that can be solubilised in this solvent (presumably very low). The UV spectrum of the micelle-imiquimod solution or in pure water after 1 h is presented in Fig. 2a. The solubilization of imiquimod in the micellar solution can be clearly assessed, as shown by the typical imiquimod spectrum obtained for the micelle-imiquimod solution in the 300–330 nm range, whereas quasi no imiquimod absorbance was observed in pure water. Blank micelle solution (no imiquimod) as a control confirmed that copolymer

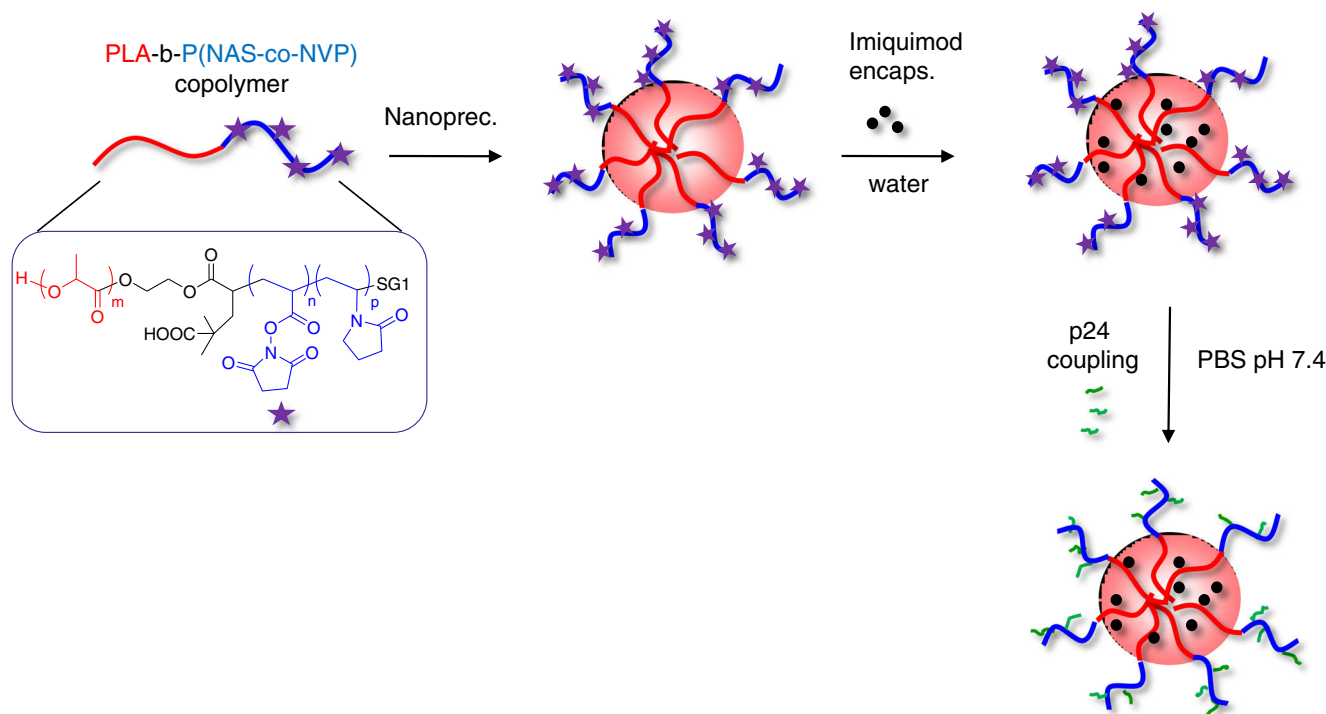


**Fig. 1** Scheme of preparation of the imiquimod/p24 loaded micelles from the PLA-b-P(NAS-co-NVP) block copolymer (SG1 = ON(<sup>t</sup>Bu)CH(<sup>t</sup>Bu)PO(OEt)<sub>2</sub>).

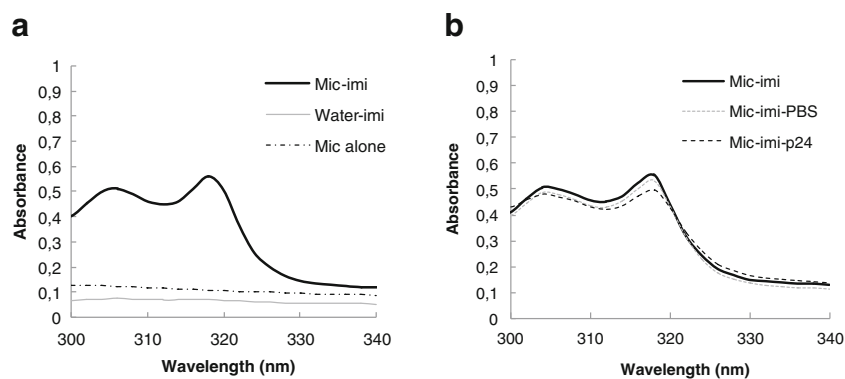


**Fig. 2** (a) UV spectra of the imiquimod loaded micelle (Mic-imi) solution ( $[Mic] = 5.2 \text{ mg.mL}^{-1}$ ), water-imiquimod solution, and reference micelle solution, after 10-fold dilution in water,  $[Mic] = 0.52 \text{ mg.mL}^{-1}$ ; (b) UV spectra of the coupling solution of imiquimod loaded micelles with p24 in PBS (Mic-imi-p24;  $[Mic] = 2.6 \text{ mg.mL}^{-1}$ ,  $[p24] = 0.3 \text{ mg.mL}^{-1}$ ) and reference imiquimod loaded micelle solution without p24 in PBS (Mic-imi-PBS;  $[Mic] = 2.6 \text{ mg.mL}^{-1}$ ) after 5-fold dilution in water ( $[Mic] = 0.52 \text{ mg.mL}^{-1}$ ); initial imiquimod loaded micelle solution (Mic-imi) is also shown as control (10-fold dilution in water,  $[micelle] = 0.52 \text{ mg.mL}^{-1}$ ).

did not interfere with UV measurements. Kinetic studies showed no further increase of absorbance for longer incubation times. To determine accurately the imiquimod loading in micelles, the micelle solution were ten-fold diluted in DMSO, to destroy the micelles, and UV absorbance observed at 318 nm. A calibration curve relying the absorbance to imiquimod concentration, established in the same conditions (DMSO/water 9/1 v/v) gave access to the concentration of imiquimod and further loading, which was found to be  $12.2 \text{ mg.g}^{-1}$  of copolymer micelle. As imiquimod contains an amino group, a control reaction of P(NAS-co-NVP) model polymer with imiquimod in water was performed, and showed that the ligand was not able to couple on the NS ester functions, most probably due to its water non-solubility. Micelle size after imiquimod loading was  $58.1 \pm 1.5 \text{ nm}$ , slightly higher than that of the non-loaded micelles.

### p24 Conjugation to the Micelle Surface

p24 was conjugated to the imiquimod loaded micelles, in PBS pH 7.4. The coupling efficiency was analyzed by SDS polyacrylamide gel electrophoresis (Fig. 3). At 0.115 mg of introduced p24 per mg of micelles ( $0.3 \text{ mg.mL}^{-1}$  p24,  $2.6 \text{ mg.mL}^{-1}$  micelles), almost no free p24 was detected, indicating that coupling was quantitative, either on the imiquimod loaded or empty micelles. This absence of interference of the ligand in the micelle corona for protein coupling strongly suggested that the ligand was mainly encapsulated into the micelles and not present at the interface. The concentration gel was kept for analysis since protein loaded micelles were too big to enter of diffuse through the gel, and could be observed at the start, as previously reported (29). The covalent character of the coupling was confirmed by the TNBS assay, revealing 90% decrease in p24 amine groups, as a result of amide formation following coupling. It is to mention that no release of

imiquimod was observed following the two-fold dilution of the micellar solution in PBS, used in p24 coupling procedure (Fig. 2b).

Following 20 h in PBS medium, either in presence or absence of p24, the micelle size significantly increased ( $\sim 100\text{--}110 \text{ nm}$ , Table I), as compared to the initially prepared micelles, whose size was  $\sim 56 \text{ nm}$ . This increase was due to the increasing hydrophilic character and thus deployment in solution of the corona following hydrolysis of the NAS pendant NS esters into negatively charged carboxylate groups that can repulse each other. This hydrolysis is competitive with the p24 coupling. For p24 conjugated micelles (with or without loaded imiquimod), the mean size was around 110 nm, compared to

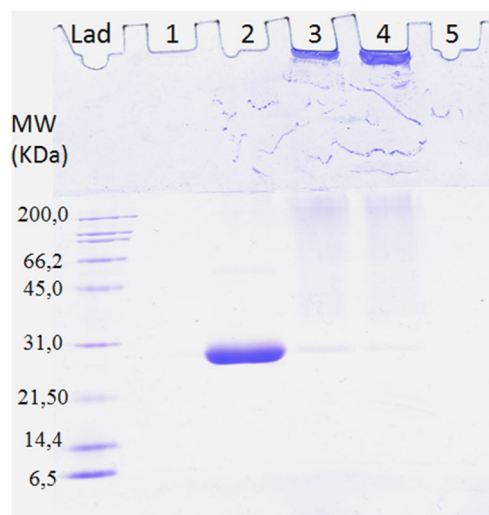


**Fig. 3** SDS PAGE analysis of p24 protein coupling on imiquimod loaded or free micelles; Lad : mass marker, 1. Control micelles loaded with imiquimod,  $[Mic-imi] = 2.6 \text{ mg.mL}^{-1}$  in PBS; 2. Free p24  $[p24] = 0.3 \text{ mg.mL}^{-1}$  in PBS; 3. Micelles conjugated to p24 (Mic-p24;  $[Mic] = 2.6 \text{ mg.mL}^{-1}$ ,  $[p24] = 0.3 \text{ mg.mL}^{-1}$ ); 4. Micelles loaded with imiquimod and conjugated to p24 (Mic-imi-p24;  $[Mic-imi] = 2.6 \text{ mg.mL}^{-1}$ ,  $[p24] = 0.3 \text{ mg.mL}^{-1}$ ), 5. Control micelles alone,  $[Mic] = 2.6 \text{ mg.mL}^{-1}$ .

**Table 1** Mean Size and Polydispersity Index (DLS) of the Micelles After Coupling of p24 in PBS pH 7.4 for 20 h; Mic and Mic-imi Control Samples Were Placed in These Coupling Conditions, in Absence of p24

Micelle code	Mean size (nm) <sup>a</sup>	PI <sup>a</sup>	Zeta potential (mV)	Loaded imi (mg/g of copolymer)	Coupled p24 (mg/g of copolymer)
Mic	99.8 ± 5.5	0.03 ± 0.01	-30.5 ± 2.3	–	–
Mic-imi	101.6 ± 3.7	0.05 ± 0.01	-29.8 ± 1.8	12.2	–
Mic-p24	111.3 ± 5.1	0.04 ± 0.01	-31.5 ± 2.5	–	115
Mic-imi-p24	110.7 ± 2.2	0.06 ± 0.02	-31.0 ± 2.0	12.2	115

<sup>a</sup> Determined by dynamic light scattering

100 nm for micelles not functionalized with p24 (with or without loaded imiquimod) and placed in the same reaction conditions (PBS, 20 h). This significant increase in size (~10 nm) confirmed the previous SDS PAGE analysis and TNBS assay indicating p24 fixation at the micelle surface, and was also consistent with the typically reported range of protein radius of gyration in physiological conditions (30). Finally, zeta potential measurements performed on either imiquimod/p24 loaded or unloaded micelles showed similar values. Unloaded micelles exhibited a negative surface charge as expected ( $\zeta = -30.5$  mV) due to partial hydrolysis of the NS esters of the corona in PBS pH 7.4. The similar value obtained for unloaded and imiquimod loaded micelles (-29.8 mV) again strongly supported that imiquimod had no contribution at the interface and was mainly encapsulated into the micelles. As for p24 surface functionalized micelles (with or without loaded imiquimod), the zeta potential value, remaining close to -30 mV, was consistent with previously obtained results in our group for PLA nanoparticles surface coated with p24, which showed a similar value (-34 mV, in the same measurement conditions, *i.e.* dilution in NaCl 1 mM (7)). Considering the isoelectric point of the p24 (pI=5.9), the p24 had indeed a slightly negative global charge at neutral pH, conferring a still negative zeta potential to micelles after surface coupling.

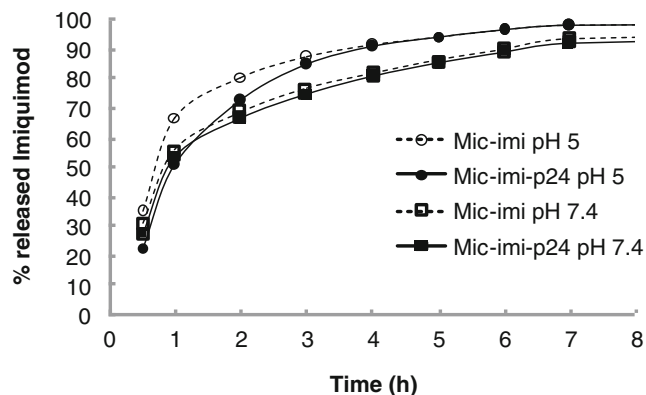


**Fig. 4** Imiquimod release from micelles conjugated or not with p24, in PBS pH 7.4 or sodium acetate pH 5 at 37°C.

## Imiquimod Release

Imiquimod release from both non functionalized and p24-functionalized micelles was then further investigated at pH 7.4 and pH 5, the latter value mimicking the pH of the intracellular endosome vesicle environment, where are localized the TLR7 receptors with which imiquimod is expected to interact. Whatever the pH, the release was rather fast with about 50% of the drug released in 1 h (Fig. 4). Earlier results in our group (7) demonstrated that the uptake of PLA based NP carriers by cells is very efficient within one hour (even in absence of ligand on the NP surface, able to specifically interact with a cell surface receptor). Thus, we can reasonably assume that the ligand encapsulated in our PLA based micelles is efficiently delivered within the cells during this short time range, and that its fast intracellular release will fit rather well with the expected action (*i.e.* binding to intracellular endosomal TLR7 receptor and further DC maturation). Interestingly, release was found slightly higher at pH 5 than pH 7.4, most probably due to the higher solubility of the imiquimod in acidic medium than in neutral one (due to protonated amine, pKa=7.3). This faster release was an interesting feature regarding the potential of imiquimod to be more efficiently released close to its TLR7 target. The surface coupled p24 did not provoke any barrier effect for imiquimod release, as compared to non-functionalized micelles.

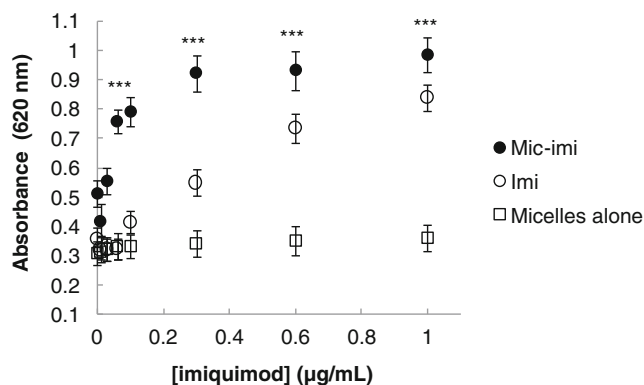


**Fig. 5** *In vitro* evaluation of the NF- $\kappa$ B and MAPK pathways activation by free or encapsulated imiquimod with RAW-Blue™ reporter cell line. Those results revealed a higher activation of the NF- $\kappa$ B and MAPK pathways when imiquimod is encapsulated into the micelles compared to the free form. Indicated values are means (SD);  $n = 3$ . ANOVA \*\*\* $P < 0.001$ .

### Enhanced NF- $\kappa$ B and MAPK Pathways Activation by the Encapsulated Imiquimod

To characterize the encapsulated TLR ligands regarding their biological function, their ability to activate the NF- $\kappa$ B signaling (31) was evaluated on RAW-Blue™ reporter cell line. As shown in Fig. 5, the co-culture of free imiquimod with RAW-Blue™ cells induces SEAP in a dose-dependent manner. Encapsulation of the ligand into PLA based micelles significantly enhanced the production of SEAP (by an amplification factor of 3 to 4), meaning an enhancement of the NF- $\kappa$ B and MAPK pathways activation ( $P < 0.001$ ).

### Enhanced Immunostimulatory Efficiency of Encapsulated Imiquimod

The maturation of DCs is one of the fundamental steps toward an effective immune response *in vivo*. We hypothesized that the intracellular fate of micelles after endocytosis could favor intracellular delivery of encapsulated ligand, increase the efficiency of imiquimod delivery into endosomal compartments expressing TLR7, and finally enhance its action. For this reason, the encapsulated imiquimod was characterized for its ability to stimulate human MoDCs maturation *in vitro*. The expression of the well-known maturation marker CD83 and

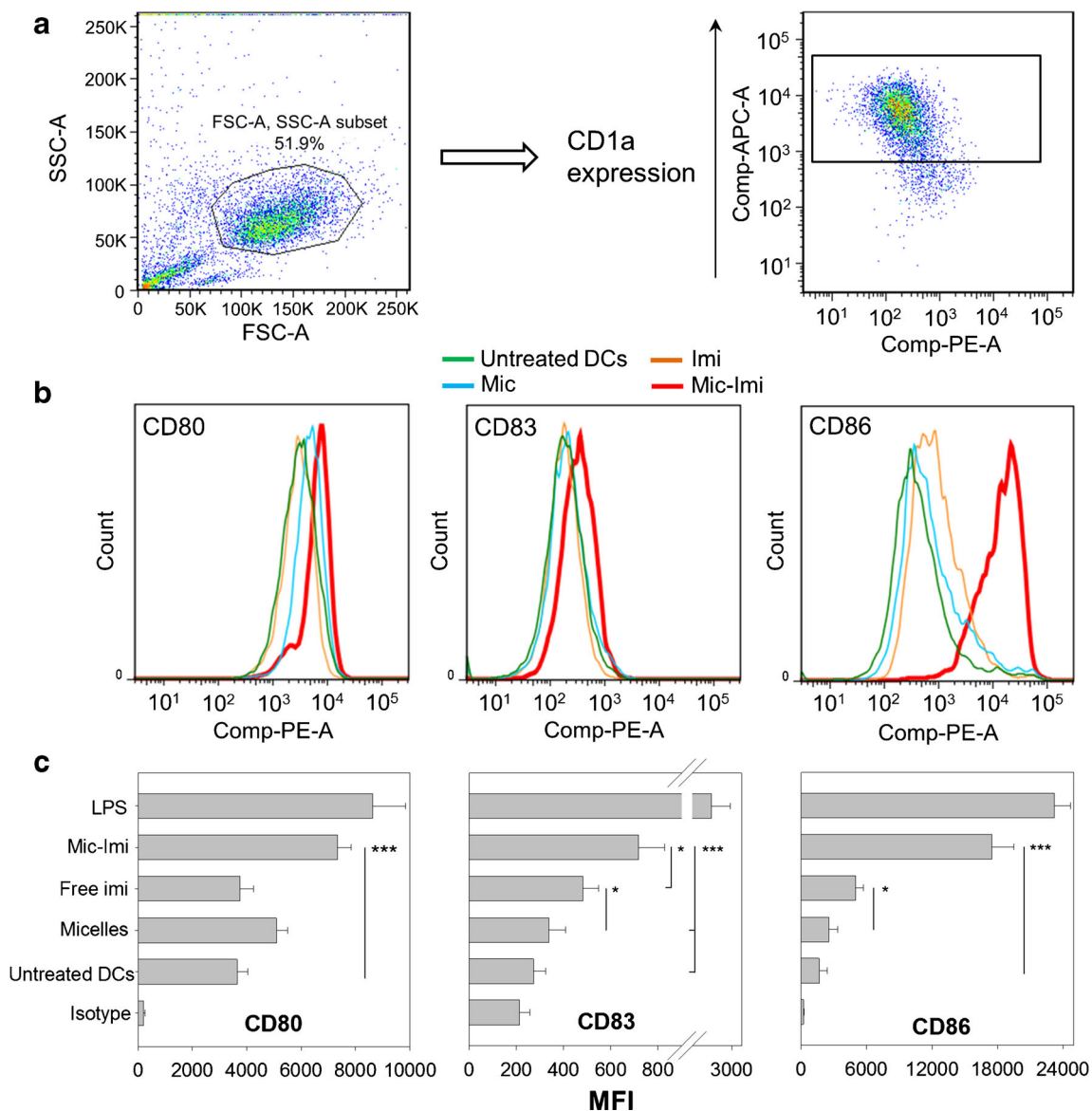


**Fig. 6** Surface expression of maturation-related molecules by human MoDCs upon exposure to free or encapsulated imiquimod, determined by flow cytometry. **(a)** Gated CD1a positive-DC population analyzed. **(b)** Histogram representation of MoDCs after phenotypes 24 h of stimulation. One experiment out of three is shown. **(c)** Mean surface expression of maturation marker CD83 and costimulatory molecules CD80 and CD86 by MoDCs upon exposure to free or encapsulated imiquimod and comparison with LPS as positive control of maturation, and empty micelles and untreated DCs as negative controls. Means (SD);  $n = 3$ . ANOVA \* $P < 0.05$ , \*\*\* $P < 0.001$ .

the costimulatory molecules CD80 and CD86 were measured. Blood derived human monocytes were isolated and cultured in the presence of GM-CSF and IL-4 during 6 days to obtain immature DCs which showed typical spiky cell membrane projections, and were characterized by the expression of CD1a and a weak expression of CD80, CD83 and CD86. Cells were stimulated with imiquimod encapsulated or not, and the impact on cell viability was investigated by propidium iodide labeling 48 h after stimulation. Untreated MoDCs and empty PLA micelles were used as reference for the immature state and MoDCs treated with LPS as control for matured MoDCs. For 5  $\mu\text{g}$  of ligands per  $10^6$  cells, a low cell death from 5% to 12% was observed after 48 h (Supplementary Fig. S1). The used imiquimod concentration of 5  $\mu\text{g}/\text{mL}$  was chosen on the basis of earlier thorough studies on this ligand regarding *in vitro* DC maturation (32,33). These studies demonstrated that DC maturation was imiquimod dose dependant, and that the optimal dose was 5  $\mu\text{g}/\text{mL}$ .

Expression of the cell surface markers CD80, CD83 and CD86 was assessed by immunofluorescence and flow cytometry 24 h poststimulation (Fig. 6). CD83 and CD86 were significantly increased on cells stimulated with free imiquimod ( $P < 0.05$ ), while empty micelles induce a low, not statistically significant DCs maturation. The expression of the three markers was significantly improved with encapsulated imiquimod ( $P < 0.001$ ) (Fig. 6). Indeed, Mic-imi significantly increased the mean of fluorescence intensity (MFI) of cells expressing CD80, CD83 and CD86 in comparison with free imiquimod by a factor 2, 1.5 and 3.5 respectively (Fig. 6c). We demonstrated that encapsulation of imiquimod into PLA micelles improves its immuno-stimulatory properties, probably due to a reduced degradation in culture medium and an improved cellular uptake and delivery to the specific

endosomal TLR7. Indeed, as shown in Fig. 4, the imiquimod release from micelles is fast at pH 5 mimicking the pH of intracellular endosomes. This observation could explain the quick and potent immunostimulatory effect of the Mic-imi observed on the MoDCs.

Previous observations shown that encapsulation of TLR (34,35) or NOD1/2 (7,36) receptor ligands into PLA/PLGA particles potentiates their immune properties. Our results confirm these observations, but with micellar preparations.

Moreover, as shown in Fig. 7, the immobilization of the p24 antigen (HIV-1) on the micelles did not change the immunostimulatory properties of the encapsulated imiquimod on MoDCs, meaning the possibility to efficiently carry both the vaccinal antigen and the immunostimulatory molecule for further *in vivo* immunization studies.

## CONCLUSIONS

Here, we developed a new generation of vaccine adjuvants based on micelles with a PLA core and a NVP based corona with pendant reactive N-succinimidyl ester moieties. Those structures allowed encapsulation of an immunostimulatory molecule (imiquimod, TLR7 ligand) as well as surface functionalization with a capsid protein of HIV-1 (Gag p24). The micelle-encapsulated imiquimod induced a stronger stimulation of human DCs than the free imiquimod. In addition, Raw-Blue cell experiments showed that the encapsulation of the ligand into the micelles enhanced the activation of the NF- $\kappa\text{B}$  and MAPK pathways. Finally, p24 antigen coupled to the micelle surface did not modify the immunostimulatory properties of encapsulated imiquimod. We conclude that this

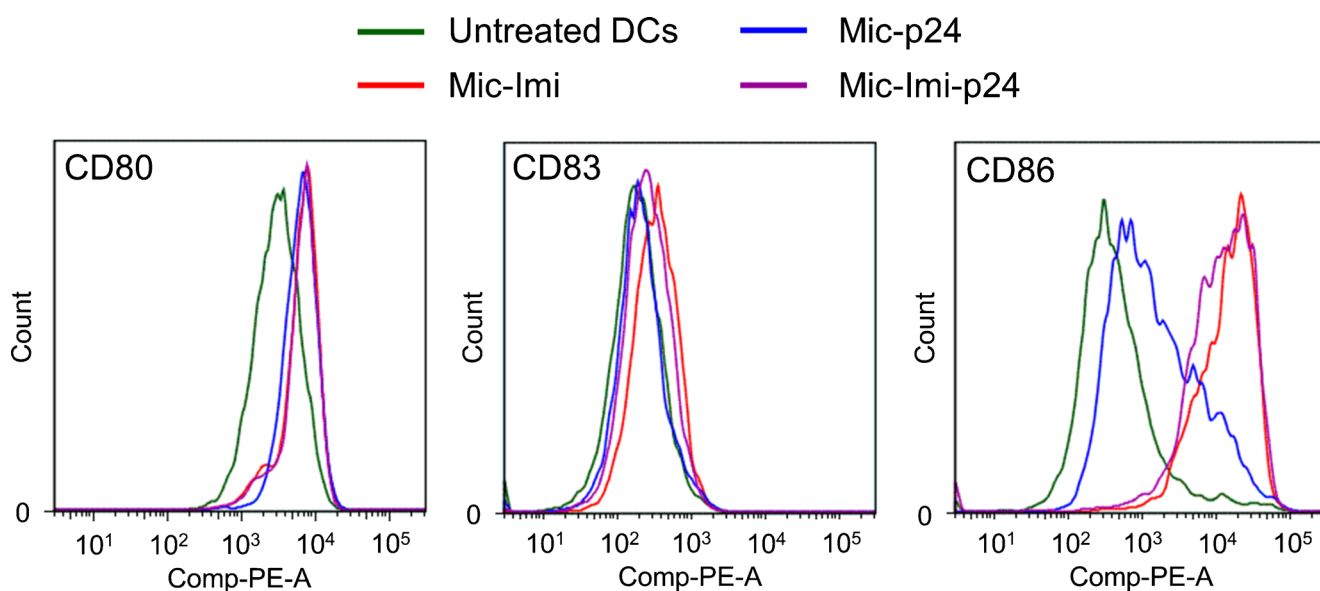


**Fig. 7** Influence of the immobilization of the p24 antigen (HIV-1) on the immunostimulating properties of encapsulated imiquimod.



micellar system, with its enhanced properties of immunostimulation, represents a promising adjuvant platform that can be readily extended to other antigens and hydrophobic ligands of interest.

## ACKNOWLEDGMENTS AND DISCLOSURES

This work was funded by the ANR (French National Research Agency) through Euronanomed grant (iNanoDCs) and ANabio research projects, and Fondation Recherche Médicale (FRM) to Vincent Pavot. This work was also partially supported by grants from the two FP7 European grants CUTHIVAC (no 241904) and ADITEC (no 280873). The funders had no role in the study design, data collection and analysis, decision to publish, or preparation of the manuscript.

## REFERENCES

- Alving CR, Peachman KK, Rao M, Reed SG. Adjuvants for human vaccines. *Curr Opin Immunol.* 2012;24:310–5.
- Kool M, Fierens K, Lambrecht BN. Alum adjuvant: some of the tricks of the oldest adjuvant. *J Med Microbiol.* 2012;61:927–34.
- Gregoriadis G, McCormack B, Obrenovic M, Saffie R, Zadi B, Perrie Y. Liposomes as immunological adjuvants and vaccine carriers. *Methods.* 1999;19:156–62.
- Fox CB, Haensler J. An update on safety and immunogenicity of vaccines containing emulsion-based adjuvants. *Expert Rev Vaccines.* 2013;12:747–58.
- Rice-Ficht AC, Arenas-Gamboa AM, Kahl-McDonagh MM, Ficht TA. Polymeric particles in vaccine delivery. *Curr Opin Microbiol.* 2010;13:106–12.
- Kasturi SP, Skountzou J, Albrecht RA, Koutsonanos D, Hua T, Nakaya HI, *et al.* Programming the magnitude and persistence of antibody responses with innate immunity. *Nature.* 2011;470:543–50.
- Pavot V, Rochereau N, Primard C, Genin C, Perouzel E, Lioux T, *et al.* Encapsulation of Nod1 and Nod2 receptor ligands into poly(lactic acid) nanoparticles potentiates their immune properties. *J Control Release.* 2013;167:60–7.
- Guillon C, Mayol K, Terrat C, Compagnon C, Primard C, Charles MH, *et al.* Formulation of HIV-1 Tat and p24 antigens by PLA nanoparticles or MF59 impacts the breadth, but not the magnitude, of serum and faecal antibody responses in rabbits. *Vaccine.* 2007;25:7491–501.
- Ataman-Onal Y, Munier S, Ganée A, Terrat C, Durand PY, Battail N, *et al.* Surfactant-free anionic PLA nanoparticles coated with HIV-1 p24 protein induced enhanced cellular and humoral immune responses in various animal models. *J Control Release.* 2006;112:175–85.
- Kawai T, Akira S. The role of pattern-recognition receptors in innate immunity: update on Toll-like receptors. *Nat Immunol.* 2010;11:373–84.
- Geddes K, Magalhães JG, Girardin S. Unleashing the therapeutic potential of NOD-like receptors. *Nat Rev Drug Discov.* 2009;8:465–79.
- Reddy ST, Swartz MA, Hubbell JA. Targeting dendritic cells with biomaterials. *Trends Immunol.* 2006;27:573–9.
- Kazzaz J, Singh M, Ugozzoli M, Chesko J, Soenawan E, O'Hagan DT. Encapsulation of the immune potentiators MPL and RC529 in PLG microparticles enhances their potency. *J Control Release.* 2006;110:566–73.
- Hafner AM, Corthésy B, Merkle HP. Particulate formulations for the delivery of poly(I:C) as vaccine adjuvant. *Adv Drug Deliv Rev.* 2013;65:1386–99.
- Schlosser E, Mueller M, Fischer S, Basta S, Busch DH, Gander B, *et al.* TLR ligands and antigen need to be coencapsulated into the same biodegradable microsphere for the generation of potent cytotoxic T lymphocyte responses. *Vaccine.* 2008;26:1626–37.
- Fievez V, Plapied L, des Rieux A, Pourcelle V, Freichels H, Wascotte V, *et al.* Targeting nanoparticles to M cells with non-peptidic ligands for oral vaccination. *Eur J Pharm Biopharm.* 2009;73:16–24.
- Beutner KR, Spruance SL, Hougham AJ, Fox TL, Owens ML, Douglas Jr JM. Treatment of genital warts with an immune response. *J Am Acad Dermatol.* 1998;38:230–9.
- Miller RL, Gerster JF, Owens ML, Slade HB, Tomai MA. Imiquimod applied topically: a novel immune response modifier and new class of drug. *Int J Immunopharmacol.* 1999;21:1–14.
- Larange A, Antonios D, Pallardy M, Kerdine-Romer S. TLR7 and TLR8 agonists trigger different signaling pathways for human dendritic cell maturation. *J Leukoc Biol.* 2009;85:673–83.
- Bachelder EM, Beaudette TT, Broaders KE, Frechet JM, Albrecht MT, Mateczun AJ, *et al.* In vitro analysis of acetalated dextran microparticles as a potent delivery platform for vaccine adjuvants. *Mol Pharm.* 2010;7:826–35.
- Handké N, Lahaye V, Bertin D, Delair T, Verrier B, Gignes D, *et al.* Elaboration of glycopolymer-functionalized micelles from an N-vinylpyrrolidone/lactide-based reactive copolymer platform. *Macromol Biosci.* 2013;13:1213–20.
- Handké N, Fichoux D, Rollet M, Delair T, Mabrouk K, Bertin D, *et al.* Lysine-tagged peptide coupling onto polylactide nanoparticles coated with activated ester-based amphiphilic copolymer: a route to highly peptide-functionalized biodegradable carriers. *Colloids Surf B: Biointerfaces.* 2013;103:298–303.
- Le Garrec D, Gori S, Luo L, Lessard D, Smith DC, Yessine MA, *et al.* Poly(N-vinylpyrrolidone)-block-poly(D, L-lactide) as a new polymeric solubilizer for hydrophobic anticancer drugs: in vitro and in vivo evaluation. *J Control Release.* 2004;99:83–101.
- Gaucher G, Asahina K, Wang J, Leroux JC. Effect of poly(N-vinyl-pyrrolidone)-block-poly(D, L-lactide) as coating agent on the opsonization, phagocytosis, and pharmacokinetics of biodegradable nanoparticles. *Biomacromolecules.* 2009;10:408–16.
- Reddy ST, Rehor A, Schmoekel HG, Hubbell JA, Swartz MA. In vivo targeting of dendritic cells in lymph nodes with poly(propylene sulfide) nanoparticles. *J Control Release.* 2006;112:26–34.
- Reddy ST, van der Vlies AJ, Simeoni E, Angeli V, Randolph GJ, O'Neil CP, *et al.* Exploiting lymphatic transport and complement activation in nanoparticle vaccines. *Nat Biotechnol.* 2007;25:1159–64.
- Eby JK, Dane KY, O'Neil CP, Hirose S, Swartz MA, Hubbell JA. Polymer micelles with pyridyl disulfide-coupled antigen travel through lymphatics and show enhanced cellular responses following immunization. *Acta Biomater.* 2012;8:3210–7.
- Tong J, Luxenhofer R, Yi X, Jordan R, Kabanov AV. Protein modification with amphiphilic block copoly(2-oxazoline)s as a new platform for enhanced cellular delivery. *Mol Pharm.* 2010;7:984–92.
- Heffernan MJ, Murthy N. Disulfide-crosslinked polyion micelles for delivery of protein therapeutics. *Ann Biomed Eng.* 2009;37:1993–2002.
- Hong L, Jinzhi L. Scaling law for the radius of gyration of proteins and its dependence on hydrophobicity. *J Polym Sci B Polym Phys.* 2009;47:207–14.

31. Schon MP, Schon M. Imiquimod: mode of action. *Br J Dermatol*. 2007;157:8–13.
32. Zhu KJ, Cen JP, Lou JX, Wang Q, Zhang X, Xu Y, *et al*. Imiquimod inhibits the differentiation but enhances the maturation of human monocyte-derived dendritic cells. *Int Immunopharmacol*. 2009;9:412–7.
33. Burns RP, Ferbel B, Tomai M, Miller R, Gaspari AA. The imidazoquinolines, imiquimod and R-848, induce functional, but not phenotypic, maturation of human epidermal langerhans' cells. *Clin Immunol*. 2000;94:13–23.
34. Wischke C, Zimmermann J, Wessinger B, Schendler A, Borchert HH, Peters JH, *et al*. Poly(I:C) coated PLGA microparticles induce dendritic cell maturation. *Int J Pharm*. 2009;365:61–8.
35. Tacke PJ, Zeelenberg IS, Cruz IJ, van Hout-Kuijter MA, van de Glind G, Fokink RG, *et al*. Targeted delivery of TLR ligands to human and mouse dendritic cells strongly enhances adjuvanticity. *Blood*. 2011;118:6836–44.
36. Wischke C, Mathew S, Roch T, Frentsch M, Lendlein A. Potential of NOD receptor ligands as immunomodulators in particulate vaccine carriers. *J Control Release*. 2012;164:299–306.